

# Hierarchically Porous Bio-Based Sustainable Conjugate Sponge for Highly Selective Oil/Organic Solvent Absorption

Rohith K. Ramakrishnan, Vinod V. T. Padil,\* Marcela Škodová, Stanisław Wacławek, Miroslav Černík,\* and Seema Agarwal\*

This paper describes a novel conjugate biodegradable sponge based on the tree gum kondagogu with excellent selective oil/organic solvent absorption ability. The conjugate sponge is made hydrophobic (water contact angle 133°) by post-process vapor phase silylation, has porosity of  $\approx 94\%$  with very low density ( $18.4 \text{ mg cm}^{-3}$ ). The sponge can absorb selectively up to 19–43 times its weight of oils and organic solvents. Meanwhile, good reusability is also observed in up to at least 10 cycles. The biodegradation behavior is studied from BOD (biological oxygen demand) analysis, where the non-silylated and silylated sponges degraded over 28 days by 92% and 76%, respectively, in waste-water sludge. The novel conjugate bio-based and biodegradable sponge used in this study is a promising sustainable material for clearing oil spills and for water treatment.

## 1. Introduction

Severe environmental and ecological problems created due to oil pollution are a global concern.<sup>[1]</sup> Although biodegradation, burning, mechanical collection, and chemical treatment are some of the most common methods employed for cleaning oil pollutants from water, the collection of oil with porous absorbent materials is highly efficient, convenient, and without the risk of secondary pollution.<sup>[2,3]</sup> For practical and industrial usage, the sorbent should show 1) high selectivity for oil in comparison to

water, 2) oil absorption capacity, 3) fast oil uptake, 4) reusability, and 5) mechanical strength for reuse, as well as environmental friendliness and low cost.<sup>[4]</sup>

Open-cell porous materials, also known as sponges, can be the ideal oil absorbents due to their simple fabrication methods, low density, large pore volume, porosity, and superabsorbent capacity.<sup>[5–7]</sup> However, commercially used polypropylene has limited sorption capability (less than  $10 \text{ g g}^{-1}$ ) and non-biodegradability.<sup>[8]</sup> Traditional inorganic sponges, such as silica sponges, are too brittle, and carbon-based sponges,<sup>[9]</sup> graphene oxide (GO) sponges,<sup>[10]</sup> magnetic PDA (polydopamine)-coated MF (melamine-formaldehyde) sponges,<sup>[11]</sup> 3D-SiO<sub>2</sub>

electrospun nanofibers-PMF (poly(melamine-formaldehyde)/LDH (layered double hydroxide) sponges,<sup>[12]</sup> and MS@PIDO (melamine sponge @poly(imide dioxime)/Alg (alginate) hybrid sponges<sup>[13]</sup> require expensive equipment, processing under harsh conditions, and sophisticated technologies, which restricts their practical applications.<sup>[14,15]</sup> In contrast, natural organic sorbents and polysaccharides, including alginate,<sup>[16]</sup> sawdust,<sup>[17]</sup> corn straw,<sup>[18]</sup> and wood chips,<sup>[19]</sup> are sustainable alternatives for the removal of oil from water. Other advantages include recyclability, recoverability of oils and chemicals, their relatively easy disposal, and degradability. However, the presence of hydroxyl groups in natural polysaccharides makes them amphiphilic, which in turn leads to poor selectivity for the adsorption of oil and hydrophobic compounds.<sup>[20–22]</sup> Hence, there is a need to study new and modified sponge materials with promising properties.


Tree exudate gums are naturally occurring polysaccharide biopolymers, which are endowed with excellent gel-forming ability, although in a pristine form, they are not suitable for oil absorption from an aqueous environment due to their higher hydrophilicity and brittleness.<sup>[23]</sup> In fact, they absorb water to make a hydrogel. Consequently, feasible approaches to enhancing their hydrophobicity, for example, by surface functionalization with hydrophobic molecules such as organosilicon compounds, are in high demand.<sup>[24,25]</sup>

Here we report the preparation and use of sustainable hydrophilic biopolymers gum kondagogu (GK) and sodium alginate (SA) for the fabrication of a reusable, hydrophobic, flexible, and ultralightweight ( $18 \text{ mg cm}^{-3}$ ) conjugate sponge for the selective and efficient separation of oil and organic solvents from aqueous

R. K. Ramakrishnan, Dr. V. V. T. Padil, M. Škodová,  
Dr. S. Wacławek, Prof. M. Černík  
Institute for Nanomaterials

Advanced Technologies and Innovation (CXI)  
Technical University of Liberec (TUL)  
Studentská 1402/2, Liberec 461 17, Czech Republic  
E-mail: vinod.padil@tul.cz; miroslav.cernik@tul.cz

Prof. S. Agarwal  
Macromolecular Chemistry II, Bavarian Polymer Institute  
University of Bayreuth  
Universitätsstraße 30, Bayreuth 95447, Germany  
E-mail: agarwal@uni-bayreuth.de

 The ORCID identification number(s) for the author(s) of this article can be found under <https://doi.org/10.1002/adfm.202100640>.

© 2021 The Authors. Advanced Functional Materials published by Wiley-VCH GmbH. This is an open access article under the terms of the Creative Commons Attribution License, which permits use, distribution and reproduction in any medium, provided the original work is properly cited.

DOI: 10.1002/adfm.202100640

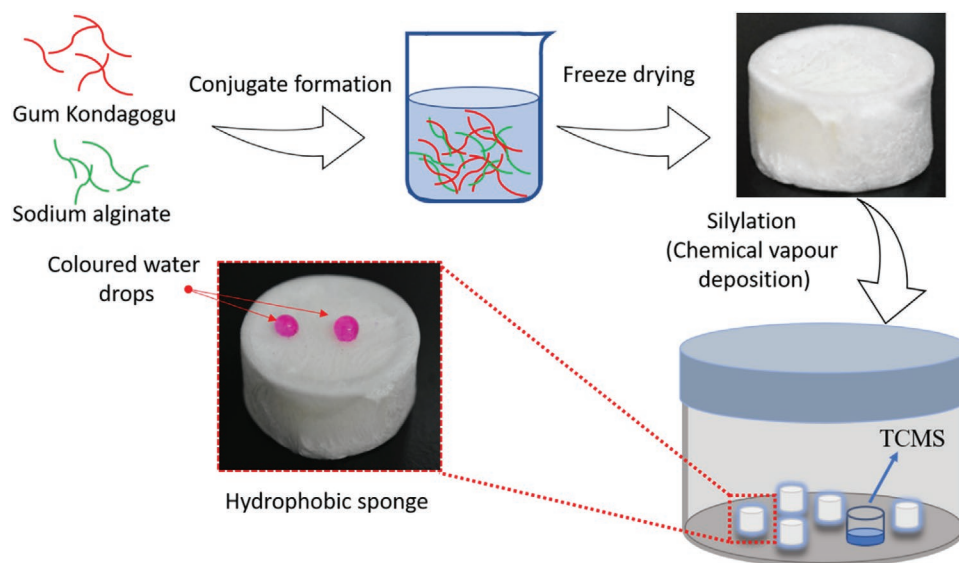


**Figure 1.** The fabrication of a conjugate GK/SA sponge and the silylation process by the chemical vapor deposition of TCMS on its surface is shown here.

solution mixture. Gum kondagogu, a cheap and sustainable polysaccharide, alone does not make a mechanically stable sponge due to its brittle nature. The non-toxic gum kondagogu, exudated from *Cochlospermum gossypium*, containing uronic acid, glucuronic acid, galacturonic acid, and low amounts of proteins, etc., has plentiful functional groups such as hydroxyl, acetyl, carbonyl, and carboxylic, which expedite network formation with other biopolymers. It can form a conjugate with sodium alginate, which is another polysaccharide comprised of two repeating, mannuronic acid and guluronic acid monosaccharide units, showing excellent liquid-gel behavior in an aqueous environment. The similarities in the basic structural units of these polysaccharides lead to the formation of a sponge with excellent mechanical properties. The method of conjugate sponge preparation as the first step is elaborated. Furthermore, silylation from the vapor phase may be performed to change the surface wetting behavior of sponges to make them suitable for selective absorption of oil, that is, hydrophilicity to hydrophobicity and oleophilic transition. The optimized silylation process provided homogeneous modification of the conjugate sponge. Hydrophobically modified sponges show selectivity for the absorption of several organic solvents and oils of different viscosities from water mixture in a short period of time for several different cycles. The bio-based polysaccharide-based biodegradable conjugate sponges with high oil/organic solvent-water absorption selectivity and after-use biodegradation provide a sustainable solution to environmental protection against oil spills and pollution.

## 2. Results and Discussion

### 2.1. GK/SA Sponge Preparation Procedure

The optimal proportions of GK and SA for obtaining a stable sponge were examined by the preparation of 11 samples with a decreasing ratio of GK to SA. From pure GK, the produced sponge has no stable structure (Figure S1, Supporting Information). In a GK/SA mixture, due to the interaction between GK and

SA, the structural integrity is formed, and the stability is proportional to SA addition. Similarly, the bulk density of the sponges was found to increase with an increasing proportion of SA (Figure S2, Supporting Information). Between 10% and 50%, there is only a slight increment in density (from 17.0 to 18.4 mg cm<sup>-3</sup>), but after that, the density rises steeply (to more than 30 mg cm<sup>-3</sup> for pure SA). Therefore, we used a GK to SA ratio of 1:1 for further studies, considering the lowest density with sufficient structural integrity. The synthesis of the GK/SA sponge and the silylation process is illustrated in **Figure 1**.

### 2.2. Morphology

The digital photograph of an optimized GK/SA sponge (**Figure 2A**) and a sponge on Foxtail grass is shown in **Figure 2B**. The ultra-light weighing character results from the GK/SA sponges morphology examined by scanning electron microscopy (SEM) (**Figure 2C,E**). This highly porous and open channel oriented structure is formed during freeze-drying by the space left after ice sublimation.<sup>[26]</sup> The cells are highly regular compared to the irregular topology of alginate sponge reported in the past,<sup>[27]</sup> probably due to the GK-SA conjugate formation. According to Tang et al.,<sup>[28]</sup> oriented open cells enhance the mechanical robustness of the pore structure. The formed porous structure is well-preserved and is not affected by the trichloromethylsilane (TCMS) hydrophobic modification (**Figure 2D,F**), which overcomes the previously observed limitation of the aqueous silylation process.<sup>[29]</sup>

The successful silylation of the GK/SA sponge was confirmed by the sharp Si peak on the recorded energy dispersive X-ray spectroscopy spectrum compared to the no-peak for the unmodified sponge (**Figure S3**, Supporting Information). The elemental distribution also indicates a high degree of Si homogeneity without aggregates of silane within the sponge. The advantage of the chemical vapor deposition (CVD) method with an extremely volatile TCMS is that a homogeneous Si-based hydrophobic surface is formed without significant change in the pore structure. The density increase was minor ( $21 \pm 0.5$  mg cm<sup>-3</sup>).

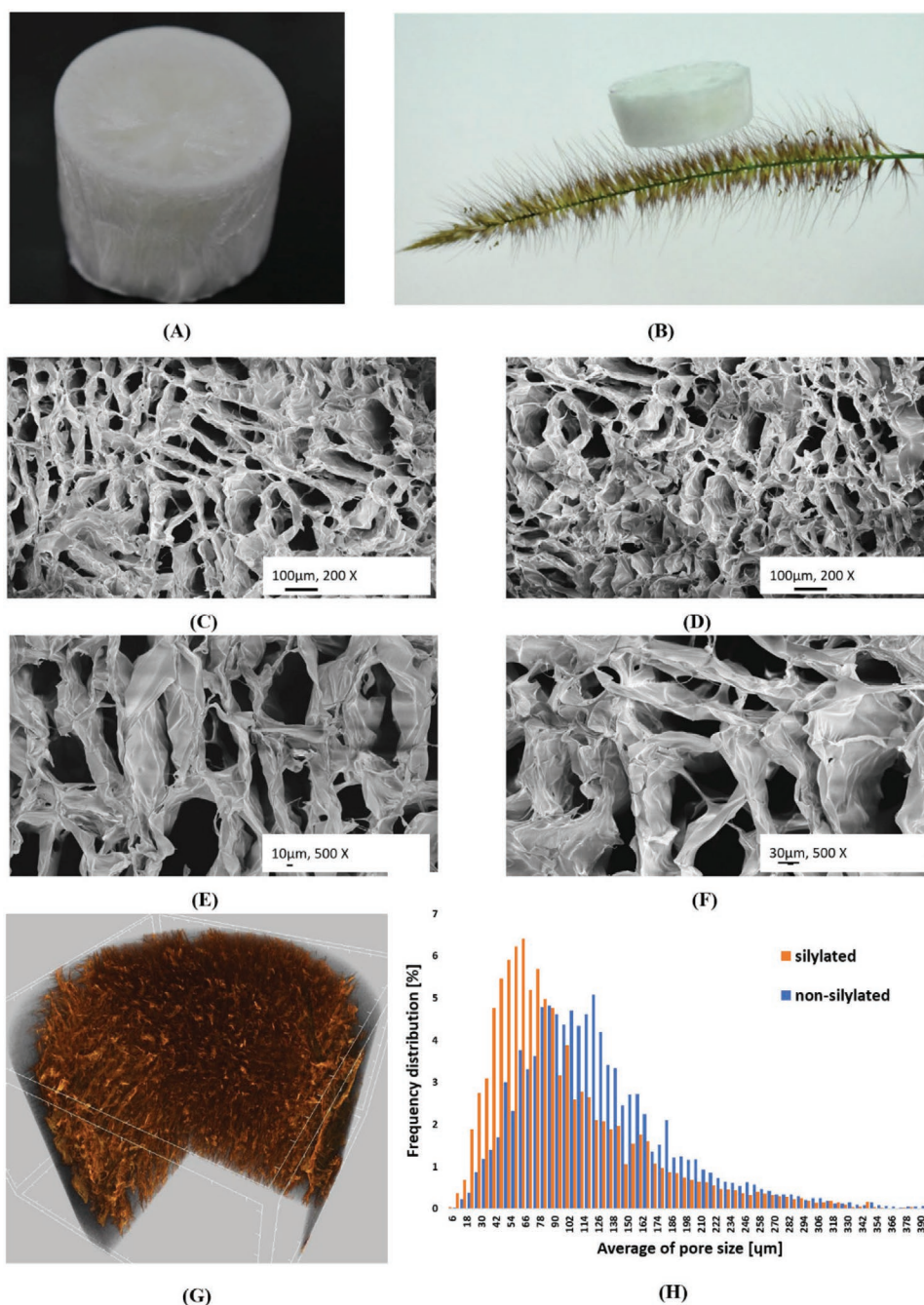


**Figure 2.** Digital photograph of the GK/SA sponge (A) kept on Foxtail grass showing the ultra-lightweight nature of the sponge (B), FE-SEM micrographs of GK/SA sponge (C,E), and silylated sponge (D,F). 3D micro-CT images of silylated sponge (G), the pore size distribution of non-silylated and silylated GK/SA sponges (H).

### 2.3. Porosity

Low bulk sponge density and high porosity are critical features that significantly influence the absorption capacity of the sponge. The microCT image of non-silylated (shown in Figure S4, Supporting Information) and silylated (Figure 2G) materials confirmed the very porous structure (in a measured range of 3 to 570 μm). The silylated sponge retains the open pore structure with only a very slight change in the porosity to 93%

(with an ommissible closed porosity of  $10^{-4}\%$ ), whereas the non-silylated material has an open porosity of 94% and a closed one again of  $10^{-4}\%$ . A determining bulk density of more than  $18.4 \pm 0.6$ ,  $\text{mg cm}^{-3}$  implies the presence of additional smaller pores, which were not determined by microCT. These microscopic and nanosized pores were formed during the swelling of the GK/SA polymer mixture and remain after silylation. When the GK and SA were added to water, the inter and intra molecular H bonding and ionic interactions bound them together,



which led to the formation of a structure where water exists in the  $\mu\text{m}$  as well as nm-sized channels/cages created by the biopolymer network. During lyophilization, water molecules were sublimed, leaving behind a porous sponge network possessing micro and nanopores.

During the silylation process, micropores are covered by silanes, and therefore their size is slightly reduced from a mean pore size of 122 to 100  $\mu\text{m}$  (Figure 2H).

## 2.4. Attenuated Total Reflection-Fourier Transform Infrared Analysis

Fourier transform infrared (FTIR) spectroscopy provides information about the molecular structure and is useful for the characterization of biopolymers (Figure S5, Supporting Information). The detailed FTIR peak correlations with the biopolymer structure are provided in the Supporting Information. The abundant hydroxyl groups on the GK/SA sponge matrix created the hydrophilic character of the sponge. Subsequently, these groups may be used in the silylation that leads to surface hydrophobicity by reaction with TCMS (Figure S7, Supporting Information).

Compared to the spectrum of the unmodified sample, the silylated sponge showed a specific absorbance at 779 and 1273  $\text{cm}^{-1}$ , assignable to the Si-CH<sub>3</sub> stretching and bending vibrations, respectively.<sup>[30,31]</sup> This alludes to the presence of methyl silane moieties and successful modification of sponge (Figure S6, Supporting Information). The Si-OH vibrations were assigned to the band at  $\approx 940\text{ cm}^{-1}$ . Furthermore, the peak at approximately 1637  $\text{cm}^{-1}$  that appeared in the silylated sample is due to the O-H bending vibrations arising from the adsorbed moisture content. Therefore, the new peaks in the spectrum imply successful silylation on the surface of the modified GK/SA sponge.

## 2.5. Water Contact Angle and Wettability

The original GK/SA sponge exhibited highly hydrophilic characteristics and a strong affinity for water. After silylation, the sponge surface became hydrophobic (and oleophilic), as confirmed by contact angle measurements with water.

Although the original sponge immediately absorbed water droplets and no measurable value was recorded (Figure 3A), the silylated sponge showed a high contact angle of 133° (Figure 3B) since the hydrophobic silicone coating formed on the surface repels water droplets.

The unmodified GK/SA sponge is amphiphilic, absorbs both the water and oil droplets immediately without any selectivity (Figure 3C). In contrast, the modified sample was very selective in terms of the absorption of oil. It showed instant wetting by the oil droplet, whereas water could not penetrate the surface (Figure 3D).

When non-silylated and silylated GK/SA sponges were placed on the water surface, the silylated sample stayed on the surface, while the non-silylated sample absorbed water and sank immediately (Figure 3E). Moreover, the hydrophilic GK/SA sponge disintegrated because of the penetration of water and collapsing the sponge structure. The silylated GK/SA sponge immersed in water showed no structural changes (Figure 3F).

## 2.6. Mechanical Properties

The mechanical properties of the non-silylated and silylated GK/SA sponges were evaluated by compression measurements. The typical stress-strain curves of the samples are shown in Figure S8, Supporting Information. The compressive stress at 20% strain of the non-silylated GK/SA sponge (6.5 kPa) was more than twice that of the alginate sponge reported earlier.<sup>[32]</sup> The notable improvement in stiffness may be closely related to the strong interaction between SA and GK through hydrogen bonding. After silylation, the compressive stress was significantly reduced due to the interrupted interaction between GK/SA. The reduction of compressive stress after silylation is assigned to two factors; one is the repulsive interactions existing between the polysiloxane methyl groups.<sup>[33]</sup> The other reason is the decrease in the degree of hydrogen bonding within the conjugate network after silylation, which leads to reduced conjugate bridge density within the material. However, the modified GK/SA sponge presented here possesses significantly more promising mechanical properties compared to other biomass-derived sponges.<sup>[34]</sup>

## 2.7. Oil and Solvent Absorption

The 3D inter-connected open pores and the goal-directed hydrophobically modified surface of the GK/SA sponge make it a promising and sustainable bio-based porous system for the removal of oils and organic solvents from water. Figure 4A,B shows its strong sorption capability for both low density (diesel oil) and high density (chloroform) solvents from water (also see Movie S1 and Movie S2, Supporting Information). When the GK/SA sponge came into contact with a diesel slick (stained with Oil Red EGN dye) floating on the water surface, it absorbed the diesel entirely within seconds without losing its form. After sorption, the sponge floated on the surface, indicating its potential use for the easy removal of oil spillages and chemical leakages. Similarly, the GK/SA sponge quickly absorbed chloroform and organic solvents denser than water (Figure 4B and Movie S2, Supporting Information). Detailed results for chloroform, ethanol, diesel, toluene, waste oil, hexane, coconut oil, and petroleum ether are shown in Table S1, Supporting Information.

The silylated bio-based GK/SA sponge showed a very high affinity for organic compounds with an absorption capacity of  $\approx 43$  times its initial weight. This high absorption capacity is comparable to carbon sponges and conjugate sponges made from the cellulose-based waste newspaper (29–51  $\text{g g}^{-1}$ )<sup>[35]</sup> and cellulose nanocrystal/poly(vinyl alcohol) sponges (32.7  $\text{g g}^{-1}$ ).<sup>[36]</sup>

The removal of oil by the sponges is mainly governed by adsorption on the surface and absorption into the bulk by capillary diffusion. The microchannels on the sponges formed during lyophilization greatly facilitate the transport of oils through the interior of the material, resulting in excellent oil absorption performance, which is illustrated in Figure 5.

## 2.8. Crude Oil Absorption Study

Crude oil spillage is one of the most common types of water contamination. Figure S9, Supporting Information, shows the absorption test using a mixture in which 2 mL of crude oil

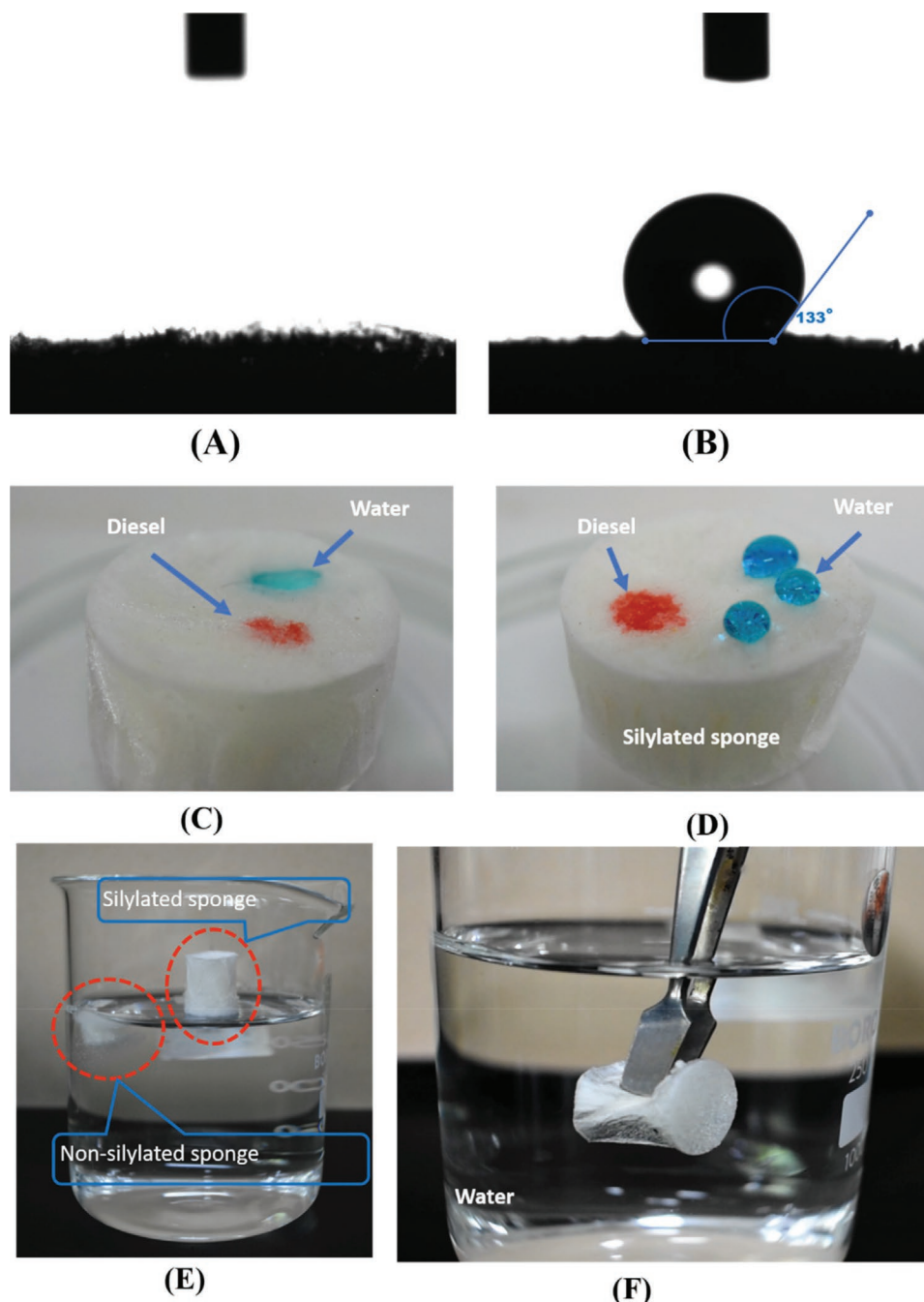


**Figure 3.** Images taken during measurement of contact angle for A) GK/SA sponge, and B) TCMS modified GK/SA sponge, C,D) Optical images of water and diesel oil droplet absorption on GK/SA sponge and TCMS modified sponge respectively, E) floating on the water surface, and F) a sample of the modified GK/SA sponge immersed in water.

was mixed with 10 mL of water. After approximately 1 min, the oil was completely absorbed (99.9%) by the GK/SA sponge (Movie S3, Supporting Information). Therefore, the kinetics of pure crude oil absorption was studied in more detail. The determined absorption is fast. In total, 23.8, 27.8, and 28.5 g g<sup>-1</sup> of crude oil were absorbed within 0.5, 1, and 2 min, respectively, which indicates the high affinity of the present sponges for the specific absorption of crude oil. The maximum absorption capacity of 28.5 g g<sup>-1</sup> achieved at 3 min is nearly double that of

state-of-the-art polypropylene fibrous mats,<sup>[8]</sup> higher than that of cellulose sponges made from waste paper (20 g g<sup>-1</sup>),<sup>[37]</sup> super-hydrophobic sawdust (17.5 g g<sup>-1</sup>),<sup>[17]</sup> and is comparable with graphene-carbon nanotube sponges (30 g g<sup>-1</sup>).<sup>[38]</sup>

## 2.9. Reusability

The reusability of the hydrophobic GK/SA sponge is advantageous for its practical application as a sustainable oil/organic

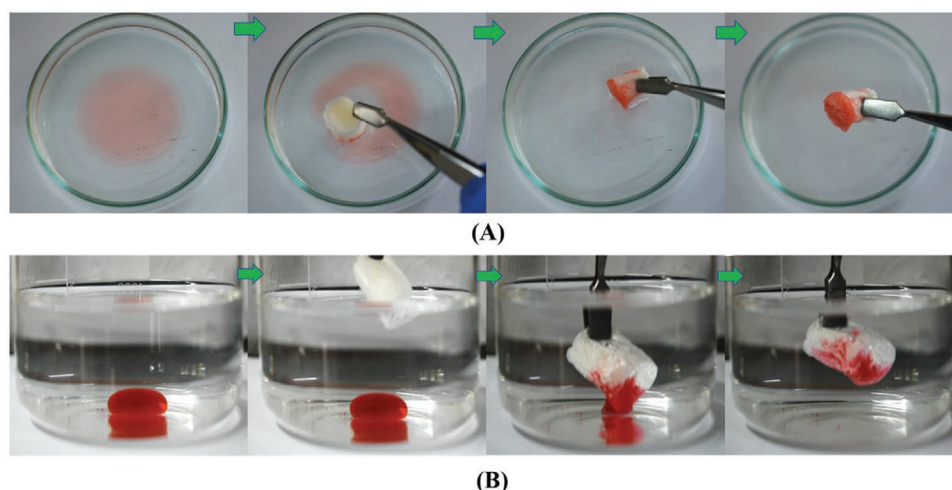


**Figure 4.** The fast and selective absorption process of diesel (A) and chloroform (B) from water by the silylated GK/SA sponge (both diesel and chloroform are stained by the Oil Red EGN dye).

solvent absorbent. Therefore, the material was tested for repeated absorption of crude oil and diesel, as examples of high and lower viscous liquids, respectively.

Crude oil was used six times for repeated absorption and manual squeezing (Figure S11A, Supporting Information). The sample showed high absorption capacity ( $28.5 \text{ g g}^{-1}$ ) and

absorbed 1.813 g of crude oil in the first cycle. The squeezing removed only 1.548 g of the absorbed oil (squeezed ratio of 85%), and therefore 0.265 g of the oil remained absorbed. During this first squeezing, the porous structure of the sponge substantially collapsed, which was observed previously,<sup>[39]</sup> and therefore, its capacity for the second absorption was reduced. In

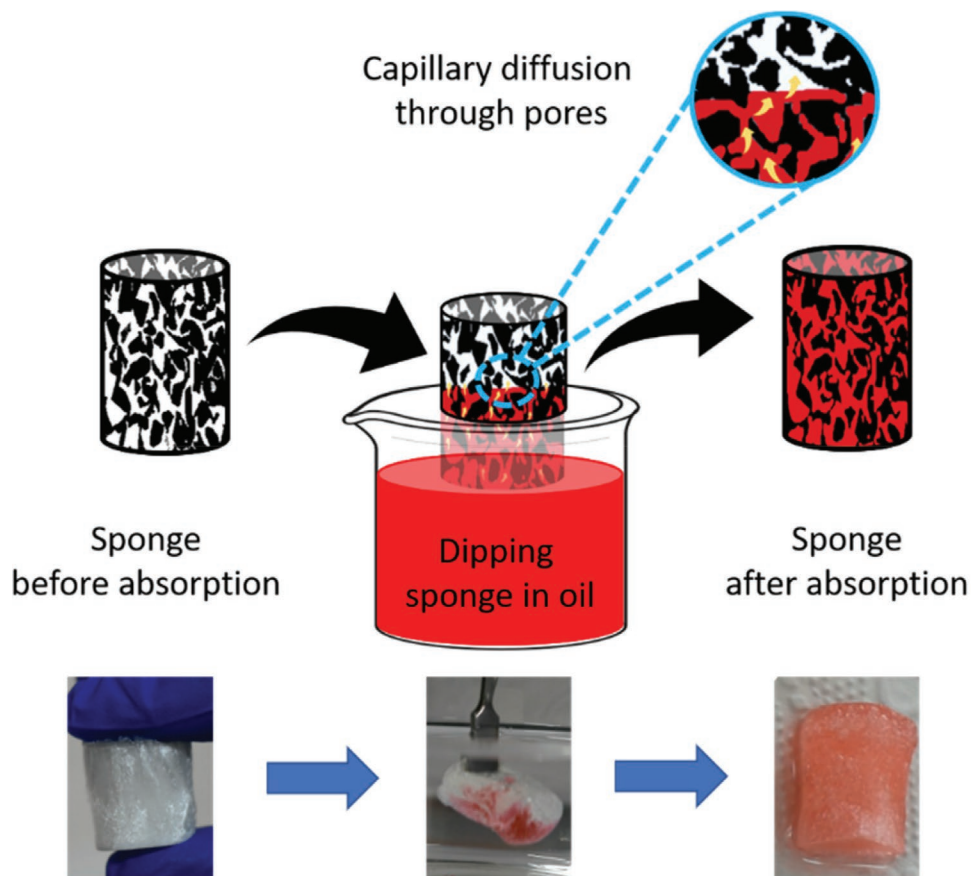


**Figure 5.** Absorption of oils by the silylated GK/SA sponge driven by capillary diffusion through the interconnected pores.

the second cycle, only 1.061 g of oil was absorbed, which gave the newly absorbed amount of  $16.7 \text{ g g}^{-1}$ , which was  $20.85 \text{ g g}^{-1}$ , including the remaining oil. The same amount (1.026 g) was squeezed back, and the squeezed ratio reached 97%. Hence, the sponge structure and its capacity were not significantly influenced by the second squeezing. Similarly, in the subsequent cycles, the absorbed amounts were slightly below 1 g ( $0.847\text{--}0.975 \text{ g}$ ), the adsorbed concentration was  $\approx 15 \text{ g g}^{-1}$ , and the squeezing ratios were roughly around 100% (98–104%). It was reported earlier that the squeezing force should not be too high to sustain the structure of the sponges.<sup>[35]</sup>

Similarly, Figure S11B, Supporting Information, shows the absorption/squeezing process for diesel up to ten cycles. Only a slight decrease in an absorbed amount from 26 to  $21 \text{ g g}^{-1}$  was determined after 10 absorptions/squeezing cycles, indicating excellent reusability performance of the GK/SA sponge as an absorbent for diesel (Figure S10, Supporting Information). Most of the bio-based sponges intended as superabsorbents lose mechanical resiliency and oil-absorption capacity after multiple absorption cycles.<sup>[40]</sup> However, the biomass-derived GK/SA sponges presented in this study maintain their mechanical integrity during ten cycles of absorption/squeezing, with diesel recovery of  $\approx 100\%$ . The reusability of sponges in oil/organic solvent absorption is directly related to its compressive stress. The material possessing high compressive stress and flexibility easily comes back to its original dimension upon removing the applied force. While performing reusability studies of the sponges by successive absorption-squeezing cycles, the oil/organic solvent absorbed in the material can easily come out of it and almost 100% porosity is available for the next cycles of absorption. Thus, high compressive strength makes the material available for a large number of cycles of absorption without compromising its structural integrity.<sup>[41]</sup>

The difference in the sponge performance for the absorption of crude oil and diesel in the absorption-squeezing cycles is due to their difference in viscosity. Crude oil has a higher viscosity than diesel. Due to the fact that a high squeezing force cannot be applied to the sponge without significantly altering its structure, it is difficult for the crude oil to extrude through the micro-channels of the sponge. Consequently, a higher amount of crude oil remains in the sample after squeezing compared to the low viscose diesel. Even after gentle squeezing of the crude oil-saturated sponge, its porosity is reduced, in contrast to squeezing of the diesel-saturated sponge.

### 2.10. Biodegradation of the Sponge

The curves of biochemical oxygen demand (BOD) analysis for the GK/SA sponge and silylated GK/SA sponge are shown in Figure S12, Supporting Information. In this process, the biopolymers are broken into smaller compounds by aerobic microbial organisms through metabolic or enzymatic processes and finally converted to carbon dioxide. The results indicating that during the whole of the measured period, BOD for GK/SA was higher than in the case of the silylated sponge. The final value of  $304.3 \pm 16.7 \text{ mg O}_2/\text{L}$  after 28 days is approximately 50% higher than the value of  $208.6 \pm 34.5 \text{ mg O}_2/\text{L}$  for the silylated sponge. The greater degradation rate of the

non-silylated sponge compared to the silylated sponge implies that the microorganisms present in the sludge may act faster on the non-silylated sponge. However, this may be influenced by the acclimatization time, the time required to produce enzymes, and the extent of biodegradation. In the early degradation stage, the carbohydrates are broken down by microorganisms into the corresponding monomers, which are glucose molecules. These monomers may either be converted to carbon dioxide and water or various other oxygenated species. The aerobes consume oxygen to oxidize substrates such as sugar in order to obtain energy. Oxygen demand is proportional to the degradation rate. The hydrophobic network of silane formed on the surface of the silylated GK/SA sponge decelerates the action of microorganisms on the material, thereby reducing the rate of degradation. Overall, the results suggest that the GK/SA sponge biodegraded more rapidly (92%) than the silylated sponge (76%) over 28 days. The conjugate sponge has higher stability against biodegradation due to a strong interaction between the polymer chains. Gum arabic bioplastic materials reported in the literature degraded completely within 15 days, whereas the GK/SA sponge took twice as long to degrade to the same extent.<sup>[42]</sup> The degradation of the GK/SA samples reported in this study is comparable to that of fiber-reinforced starch and cellulose materials.<sup>[43]</sup> The bio-based biodegradable adsorbent materials are assumed to have greater importance in industry as a green choice for reducing the amounts of waste generated as well as the cost of production. Biodegradable sponge materials of renewable resource origin could contribute to sustainable development by eliminating the possibility of secondary pollution arising due to the disposal of the sponge after the desired function. At the same time, it makes the recycling process more easily achievable.

## 3. Conclusion

In this study, a highly porous, lightweight conjugate sponge was fabricated based on renewable and biodegradable resources, polysaccharide GK and SA. Surface modification of the material was accomplished via a feasible chemical vapor deposition method using TCMS, which endowed the sponge with hydrophobic (water contact angle  $133^\circ$ ) and oleophilic properties, without altering its microporous structure or porosity. The modified GK/SA sponge was highly selective for oil and organic solvents in comparison to water and performed extremely well, showing a high absorption capacity for a wide range of oils and organic solvents (up to  $43 \text{ g g}^{-1}$ ) compared with the absorption capacities reported for many other biomass-derived sponges. At the same time, it shows good mechanical integrity and excellent reusability up to 10 cycles with a diesel absorption retention of 91% compared to the first cycle. The material undergoes biodegradation, which is a green option for reducing waste volumes after use.

## 4. Experimental Section

All experimental details regarding the materials and their characterization are provided in the Supporting Information.



**Fabrication of Conjugate Sponge:** Firstly, 1.5% (w/v) aqueous solutions of GK and SA were prepared and thoroughly mixed at various GK/SA (w/w) ratios (10:0, 9:1, 8:2, 7:3, 6:4, 5:5, 4:6, 3:7, 2:8, 1:9, and 0:10), and stirred at room temperature ( $\approx 1500$  rpm,  $22^\circ\text{C}$ ) for 2 h. The resulting GK/SA solutions were poured into a mold, frozen at  $-80^\circ\text{C}$  overnight, and lyophilized for 72 h.<sup>[44]</sup> The conjugates with different concentrations of GK and SA; 0.5, 1.0, 1.5, and 2.0% (w/v) were tried. A stable structure using 0.5% and 1.0% concentrations were not obtained, while a brittle and high-density structure has resulted in 2.0%. Considering the suitable structural stability, density and flexibility, the concentration was fixed at 1.5% (w/v).

**Hydrophobic Coating on The Conjugate Sponge:** CVD of TCMS on the GK/SA sponge was performed by placing them both into a glass bottle in an oven at  $50^\circ\text{C}$  for 30 min.<sup>[9]</sup> Subsequently, the formed silylated GK/SA sponge was placed in a vacuum oven to remove the excess TCMS from the surface of the sample.

## Supporting Information

Supporting Information is available from the Wiley Online Library or from the author.

## Acknowledgements

The authors would like to acknowledge the assistance provided by the Research Infrastructure NanoEnvicZ, supported by the Ministry of Education, Youth and Sports of the Czech Republic in the framework of Project No. LM2018124. This work was also supported by the project "Tree Gum Polymers and their Modified Bioplastics for Food Packaging Application" granted by Bavarian-Czech-Academic-Agency (BTHA) (registration numbers LTAB19007 and BTHA-JC-2019-26) and the Ministry of Education, Youth and Sports in the Czech Republic under the "Inter Excellence – Action program" within the framework of the project "Bio-based Porous 2D Membranes and 3D Sponges Based on Functionalized Tree Gum Polysaccharides and their Environmental Application" (registration number LTAUSA19091) – TUL internal No.: 18309/136. Scientific discussions with Prof. Andreas Greiner during the progress of the work are kindly acknowledged.

Open access funding enabled and organized by Projekt DEAL.

## Conflict of Interest

The authors declare no conflict of interest.

## Data Availability Statement

The data that supports the findings of this study are available in the supplementary material of this article.

## Keywords

conjugate sponge, freeze-drying, gum kondagogu/sodium alginate, oil absorption, silylation

Received: January 20, 2021

Revised: February 3, 2021

Published online: February 24, 2021

[1] W.-J. Yang, A. Chun Yin Yuen, A. Li, B. Lin, T. Bo Yuan Chen, W. Yang, H.-D. Lu, G. H. Yeoh, *Cellulose* **2019**, 26, 6449.

- [2] M. B. Wu, S. Huang, C. Liu, J. Wu, S. Agarwal, A. Greiner, Z. K. Xu, *J. Mater. Chem. A* **2020**, 8, 11354.
- [3] S. Wang, X. Peng, L. Zhong, J. Tan, S. Jing, X. Cao, W. Chen, C. Liu, R. Sun, *J. Mater. Chem. A* **2015**, 3, 8772.
- [4] H. Sai, R. Fu, L. Xing, J. Xiang, Z. Li, F. Li, T. Zhang, *ACS Appl. Mater. Interfaces* **2015**, 7, 7373.
- [5] S. Jiang, S. Agarwal, A. Greiner, *Angew. Chem., Int. Ed.* **2017**, 56, 15520.
- [6] G. Duan, S. Jiang, V. Jérôme, J. H. Wendorff, A. Fathi, J. Uhm, V. Altstädt, M. Herling, J. Brey, R. Freitag, S. Agarwal, A. Greiner, *Adv. Funct. Mater.* **2015**, 25, 2850.
- [7] S. Zhao, W. J. Malfait, N. Guerrero-Alburquerque, M. M. Koebel, G. Nyström, *Angew. Chem., Int. Ed.* **2018**, 57, 7580.
- [8] Q. F. Wei, R. R. Mather, A. F. Fotheringham, R. D. Yang, *Mar. Pollut. Bull.* **2003**, 46, 780.
- [9] M. B. Wu, S. Huang, T. Y. Liu, J. Wu, S. Agarwal, A. Greiner, Z. K. Xu, *Adv. Funct. Mater.* **2020**, 31, 2006806.
- [10] F. Liu, T. S. Seo, *Adv. Funct. Mater.* **2010**, 20, 1930.
- [11] Y. Liu, X. Wang, S. Feng, *Adv. Funct. Mater.* **2019**, 29, 1.
- [12] W. Lv, Q. Mei, J. Xiao, M. Du, Q. Zheng, *Adv. Funct. Mater.* **2017**, 27, 1.
- [13] D. Wang, J. Song, S. Lin, J. Wen, C. Ma, Y. Yuan, M. Lei, X. Wang, N. Wang, H. Wu, *Adv. Funct. Mater.* **2019**, 29, 1.
- [14] H.-Y. Mi, X. Jing, H. X. Huang, X. F. Peng, L. S. Turng, *Ind. Eng. Chem. Res.* **2018**, 57, 1745.
- [15] S. Gupta, N. H. Tai, *J. Mater. Chem. A* **2016**, 4, 1550.
- [16] R. R. Escudero, M. Robitzer, F. Di Renzo, F. Quignard, *Carbohydr. Polym.* **2009**, 75, 52.
- [17] D. Zang, F. Liu, M. Zhang, Z. Gao, C. Wang, *Chem. Eng. Res. Des.* **2015**, 102, 34.
- [18] Y. Li, X. Liu, W. Cai, Y. Cao, Y. Sun, F. Tan, *Korean J. Chem. Eng.* **2018**, 35, 1119.
- [19] Z. Zhu, S. Fu, L. A. Lucia, *ACS Sustainable Chem. Eng.* **2019**, 7, 16428.
- [20] S. Zhou, P. Liu, M. Wang, H. Zhao, J. Yang, F. Xu, *ACS Sustainable Chem. Eng.* **2016**, 4, 6409.
- [21] A. Tripathi, G. N. Parsons, O. J. Rojas, S. A. Khan, *ACS Omega* **2017**, 2, 4297.
- [22] L. Y. Long, Y. X. Weng, Y. Z. Wang, *Polymers* **2018**, 8, 1.
- [23] L. Wang, M. Sánchez-Soto, T. Abt, *Ind. Crops Prod.* **2016**, 91, 15.
- [24] J. S. Acevedo, C. Boris, I. K. Thelma, E. S. Quezada, *Pet. Sci.* **2017**, 14, 84.
- [25] J. Shi, L. Lu, W. Guo, J. Zhang, Y. Cao, *Carbohydr. Polym.* **2013**, 98, 282.
- [26] L. Wang, D. A. Schiraldi, M. Sanchez-Soto, *Ind. Eng. Chem. Res.* **2014**, 53, 7680.
- [27] H. B. Chen, Y. Z. Wang, M. Sánchez-Soto, D. A. Schiraldi, *Polymer* **2012**, 53, 5825.
- [28] P. Lv, X. Tang, R. Zheng, X. Ma, K. Yu, W. Wei, *Nanoscale Res. Lett.* **2017**, 12.
- [29] G. Chantereau, N. Brown, M. A. Dourges, C. S. R. Freire, A. J. D. Silvestre, G. Sebe, V. Coma, *Carbohydr. Polym.* **2019**, 220, 71.
- [30] A. G. Cunha, C. Freire, A. Silvestre, C. P. Neto, A. Gandini, M. N. Belgacem, D. Chaussy, D. Beneventi, *J. Colloid Interface Sci.* **2010**, 344, 588.
- [31] J. Yang, H. Li, T. Lan, L. Peng, R. Cui, H. Yang, *Carbohydr. Polym.* **2017**, 178, 228.
- [32] Y. Cheng, L. Lu, W. Zhang, J. Shi, Y. Cao, *Carbohydr. Polym.* **2012**, 88, 1093.
- [33] F. Zou, L. Peng, W. Fu, J. Zhang, Z. Li, *RSC Adv.* **2015**, 5, 76346.
- [34] S. Zhao, O. Emery, A. Wohlhauser, M. M. Koebel, C. Adlhart, W. J. Malfait, *Mater. Des.* **2018**, 160, 294.
- [35] S. Han, Q. Sun, H. Zheng, J. Li, C. Jin, *Carbohydr. Polym.* **2016**, 136, 95.
- [36] X. Gong, Y. Wang, H. Zeng, M. Betti, L. Chen, *ACS Sustainable Chem. Eng.* **2019**, 7, 11118.



- [37] S. T. Nguyen, J. Feng, N. T. Le, A. T. T. Le, N. Hoang, V. B. C. Tan, H. M. Duong, *Ind. Eng. Chem. Res.* **2013**, 52, 18386.
- [38] S. Kabiri, D. N. H. Tran, T. Altalhi, D. Losic, *Carbon* **2014**, 80, 523.
- [39] A. Tripathi, G. N. Parsons, S. A. Khan, O. J. Rojas, *Sci. Rep.* **2018**, 8, 1.
- [40] J. Jiang, Q. Zhang, X. Zhan, F. Chen, *ACS Sustainable Chem. Eng.* **2017**, 5, 10307.
- [41] C. Li, D. Jiang, H. Liang, B. Huo, C. Liu, W. Yang, J. Liu, *Adv. Funct. Mater.* **2018**, 28, 1.
- [42] V. V. T. Padil, C. Senan, S. Wacławek, M. Černík, S. Agarwal, R. S. Varma, *ACS Sustainable Chem. Eng.* **2019**, 7, 5900.
- [43] J. C. Bénézet, A. Stanojlovic-Davidovic, A. Bergeret, L. Ferry, A. Crespy, *Ind. Crops Prod.* **2012**, 37, 435.
- [44] S. Suenaga, M. Osada, *Int. J. Biol. Macromol.* **2019**, 126, 1145.